PAPER

Flexible touch sensor fabricated by double-sided nanoimprint lithography metal transfer

IOP Publishing Nanotechnology

Nanotechnology **31** (2020) 315302 (5pp) https://doi.org/10.1088/1361-6528/ab8a90

Flexible touch sensor fabricated by double-sided nanoimprint lithography metal transfer

Muyi Yang, Kai Xu and Liang Wang

Department of Optics and Optical Engineering, Anhui Key Laboratory of Optoelectronic Science and Technology, University of Science and Technology of China, No.96, JinZhai Road, Hefei 230026, Anhui, People's Republic of China

E-mail: lwang121@ustc.edu.cn

Received 12 November 2019, revised 20 March 2020
Accepted for publication 17 April 2020
Published 13 May 2020

Abstract

A double-sided nanoimprint lithography metal transfer method has been developed to fabricate a flexible capacitive touch sensor. The electrodes of this sensor are aligned and overlapped to each other and consist of a diamond aluminum mesh, which achieved a transmittance of 94% and anisotropic surface resistivity. The maximum capacitance change of the touch sensor unit is up to 41.8% when fullly touched. A 3 × 3 sensor array was tested to prove good touch detection function and the potential for large-scale applications.

Keywords: nanoimprint lithography, flexible devices, capacitive sensor

(Some figures may appear in colour only in the online journal)

1. Introduction

The rapid development of flexible devices has attraced much attention due to the enormous application potential it has shown, such as flexible displays [1], flexible biosensors [2], flexible solar cells [3] and many other devices [4]. Among the many applications, such as a crucial human-computer interaction interface, flexible touch detectors play an essential role, which increases the demands on low-cost, low resistance, high transmittance flexible conductive electrodes. Although Sn-doped In_2O_3(ITO) is the most commonly used transparent electrode in capacitive touch screen panels because of its high transmittance and electrical conductivity, some key issues such as brittleness and high electrical resistance make it impractical to use ITO in low-cost and effective flexible touch sensors [5, 6]. In order to find a replacement of conventional high-cost ITO, many materials were proposed and demonstrated good performance, such as graphene [7, 8], metal nanowires [9, 10], metal nanoparticles [11, 12], organic polymers [13–15], carbon nanotubes [16–18] an a Cu_2O-Cu-Cu_2O grid [6]. Among these materials, the metal mesh has a simple structure, stable performance, and excellent flexibility, which makes it an ideal transparent conductive material with great research value and application prospect. However, in previous research, the fineness of the metal mesh remained at a low level, which was reflected in the line width of about a few microns or a dozen microns [12, 19]. The materials used in the metal mesh were mostly copper and silver, and the cost of these materials limited the further cost reduction of metal grids [12, 19, 20]. Thus there is still a lack of an efficient way to prepare high-precision, high-performance transparent conductive electrodes using inexpensive metals to meet the needs of large-scale production. Due to its high efficiency, low cost and excellent compatibility with flexible substrates, nanoimprint lithography (NIL) shows tremendous potential for flexible device fabrication [21, 22]. Because nanoimprinting is not limited by the optical diffraction limit, it can significantly improve the processing accuracy of flexible materials. The imprinting method has evolved from plate-to-plate (P2P) to roll-to-plate (R2P) [22–24] and roll-to-roll (R2R) [25, 26]. However, due to the lack of alignment ability, conventional nanoimprinting can only perform single-sided transfer operations, which limits its further development because the widely used capacitive multi-touch devices requires two layers of electrodes.

In this work, we fabricated a touch sensor consisting of two layers of flexible transparent conductive electrodes by a new

method, double-sided nanoimprint lithography metal transfer, and tested its electrical and optical properties. Since the traditional mutual capacitance electrode structure has been extensively studied, the detector in this work was designed in such a way that the upper electrode overlaps the lower electrode. The mesh has a diamond structure, which allows it to havetransmission and electrical anisotropy. The surface resistivity is different in two mutually perpendicular directions. We studied different factors of metal mesh structures, including linewidth, period and side length. Furthermore, we measured a 3 × 3 sensor array and verified its performance as a touch detector.

2. Design and experiment

2.1. Design of the touch sensing unit

Figure 1 shows the schematic design and good transparency of the fabricated touch sensor.The proposed touch sensor has a sandwich structure based on a polyethylene terephthalate (PET) film. The electrode pads were located on both sides of the PET film and formed by diamond metal mesh. The width of each line was 1 μm, and the distance between two lines was 35 μm to ensure relatively high transmittance. The intersect angle was 60 degrees. The thickness of the PET film was about 38.5 μm, and the side length of a single square electrode was set as 2.15 mm. The upper and lower electrodes formed a capacitor structure. Using diamond mesh instead of square mesh brought two benefits. The first one was diamond mesh can lead to anisotropy of surface resistance, which means the resistance of one direction is significantly smaller than that of the other direction. Theoretically, the resistance in its smaller direction is $\sqrt{3}$ times smaller than that of the rectangular grid with the same line width and line period. Due to this property, there is an easy way to reduce or increase the resistance of the electrodes by connecting the external circuits to specific directions. The other reason was that compared with the rectangular grid, the diamond structure can provide a more considerable capacitance value in the same circumstance, which will result in a more considerable change in capacitance when the sensor is touched. As an inexpensive metal material widely used in the semiconductor industry, aluminum (Al) had been chosen as the primary conductive material for our detectors. The metal mesh consisted of 600 nm thick Al, and 20 nm thick titanium (Ti) at the bottom as an adhesion layer between the metal and PET film, making it easier to be transferred.

2.2. Fabrication of the sensor

The manufacturing process consists of six steps, as shown in figure 2(a). The process before nanoimprinting were all based on a quartz wafer because of its lower surface energy, which helped the metal transfer successfully. After cleaning, prior to fabricating the metal mesh, the anti-sticking treatment was applied to the wafer to reduce the adhesion between the metal and quartz wafer. The wafer was immersed in the heptane solution that contained 1 μl Perfluorodecyltrichlorosilane (FDTS) for 10 min and then rinsed in pure heptane. After that, the

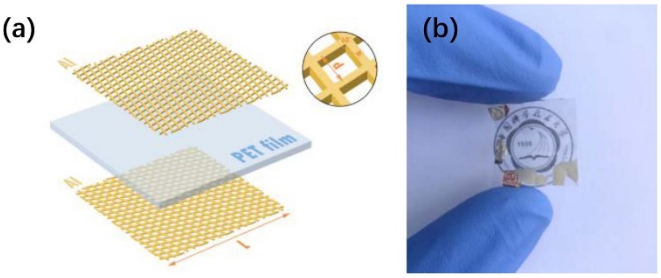

Figure 1. (a) Structure of the double layer sensor based on Al mesh. (b) Photograph of the sensor on top of an USTC logo showing its good flexibility and high transmittance.

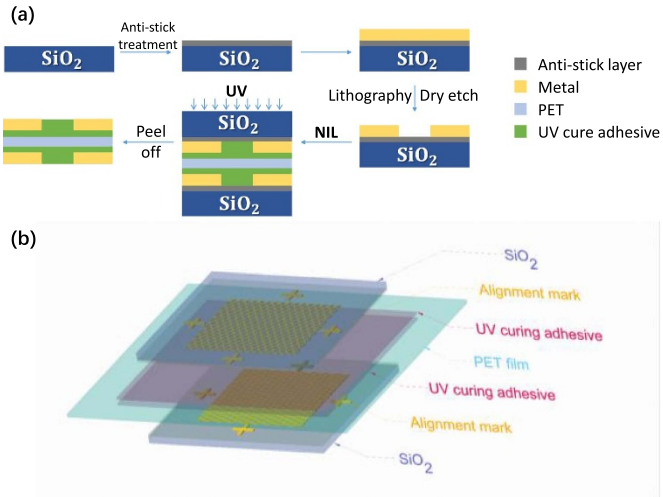

Figure 2. (a) Process flow of the double layer sensor. (b) Schematic diagram of the alignment step.

wafer was baked at 110 degrees for 10 min to finish the anti-istick treatment. It could be easily observed that the contact angle of the treated quartz with the water droplets was significantly increased, which meant that the treatment was successful. Once the treatment was finished, Al and Ti were deposited on the wafer sequentially by an Ebeam evaporator (Lesker LAB18). The metal mesh pattern and optical alignment mark were made by maskless lithography (ATD1500, AdvanTools Semiconductor Co, Ltd). After plasma etching (Oxford Instrument ICP180) and photoresist removal, the metal mesh template with the alignment mark was fully prepared.

The final and key step was to transfer the metal to PET (Mitsubishi Chemical Performance Polymers (China) Co., Ltd.) by NIL. In order to solve the misalignment problem, a microscope was installed on the original plate-to-plate imprinting system to observe the alignment marks on the upper and lower metal mesh templates. Before the start of nanoimprinting, two pieces of the above-mentioned metal-mesh templates were fixed face-to-face at the aligned position, and then PET with UV curing adhesive (Ky90fs-301E, PhiChem America, Inc.) dropped on both sides was placed between them, as shown in figure 2(b). The alignment position of the upper and lower electrodes could be further adjusted by alignment mark with a UV curing adhesive fill in. Under the pressure of 50 Pa, the whole sample was

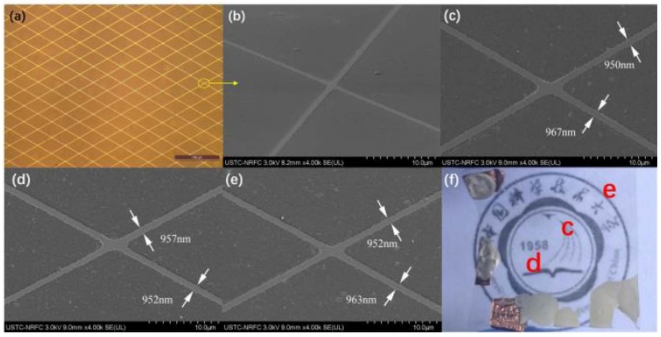

Figure 3. (a) Optical microscopic image of the Al mesh. (b). Oblique view taken by SEM. (c)~(e) SEM observation on varirous parts of the sample. (f) Location of (c)~(e) on the sample.

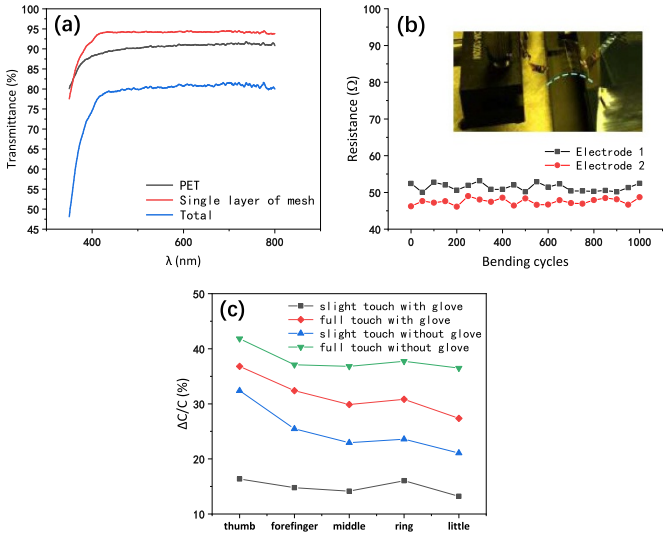

Figure 4. (a) The transmittance of single Al mesh layer, PET film and the whole sensor. (b) The resistance variation of two electrodes in bending test and the bending setup. (c) The performance of the sensor when it is touched by different fingers with and without glove.

exposed to UV light for 100 s to ensure the adhesive was entirely cured. By peeling off the quartz from PET film, the metal remained on both sides of the film so that the double-sided detectors were manufactured in one shot.

3. Result and discussion

3.1. The properties of the mesh electrode

Optical microscope observation showed that the metal transfer process succesfully moved the metal from quartz wafers to PET film and had no damage to the mesh structure, as shown in figure 3(a). Figure 3(b) is the oblique view of the metal line intersection on the PET film checked by SEM, which shows that the metal wire was embedded in UV curing adhesive, and only the upper surface was exposed for conduction to external circuits. This effect explained the robustness of the sample in the experiment, which means the sample will not be damaged by slight scratches. Fabrication uniformity has also been calibrated by cheking the center and two edges of the sensor via SEM inspection. As shown in figures 3(c) ~ (e), the line width varies from 950 nm to 967 nm, which demonstrates very good fabrication uniformity.

To characterize the degree of sample oxidation, Ellipsometer(SOPRA, GES5E) was used to measure the native oxide layer. The thickness of the native oxide layer was measured to be 6.8 nm. Since the lower surface of the Al was covered by Ti, the oxide layer was present on upper and side surface. Calculations according to Ohm's Law show that when the thickness of the oxide layer is 6.8 nm, the resistance of the electrode is about 2.5% higher than that of the electrode without oxidation. This increase in resistance may cause a slight increase in response time and power consumption, although its influnce is expected to be minimal.

The transparency of the entire touch sensor was measured by a spectrophotometer, as shown in figure 4(a). The transmittance of the whole sensor and PET film was about 81% and 91%, respectively, in a spectrum range from 350 nm to 800 nm. Since the sensor was a combination of double layers of metal mesh and PET film, the transmittance of a single layer of metal mesh was measured by setting the transmittance of PET as a baseline and extracting a root of the result, which was about 94%.

To characterize the anisotropy and conductivity of this grid, we used a four-probe method to measure the surface resistance in two directions perpendicular to each other [27]. When a current of 1 mA was injected from two adjacent corners of the mesh region, by measuring the voltage drop between the other two corners, the surface resistance in one direction was calculated by the formula $R_{\square} = \frac{\pi}{\ln 2} \cdot \frac{V}{I}$, which was 0.680 Ω/□. By rotating the mesh 90 degrees, the surface resistance in the other direction was measured as 9.517 Ω/□. There was a vast difference in surface resistivity in these two directions, and the disadvantage of relatively low Al conductivity could be compensated by selecting a direction in which the resistance was small. The surface resistance parallel to the electrodes, rather than the surface resistance in the vertical direction, has a major contribution to the resistance of the electrode in the external circuit. By increasing or decreasing the intersect angle, the resistance of the electrode can be increased or decreased due to the change of surface resistance parallel to the electrode. This could affect the performance of the sensor, such as response time and power consumption. Therefore, the electrical performance of the sensor can be adjusted by only changing the intersect angle but not affecting the metal thickness and optical transmittance.

A bending test is a good way to check the flexibility of a sample [28]. The resistance of a single electrode on both sides of PET was measured in the bending test with a bending radius of 20 mm, as shown in figure 4(b). The difference in resistance between electrodes was mainly due to the difference in contact resistance. The electrodes could maintain a relatively stable resistance even after being bent a large number of times, indicating that its metal structure had not been degraded by repeated bending cycles.

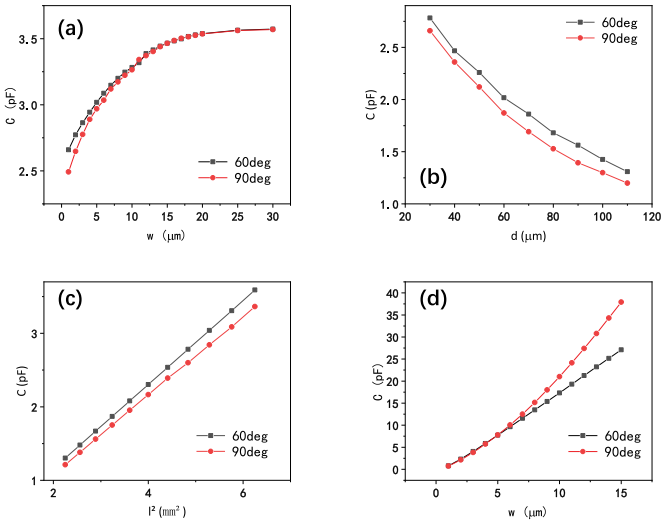

Figure 5. Simulation results of the mesh capacitance. (a)–(c) The relationship of C-w, C-d, and C-l^2, respectively. (d) The relationship between C and w when d is set as 35 times of w and the l is set as 33 times of d.

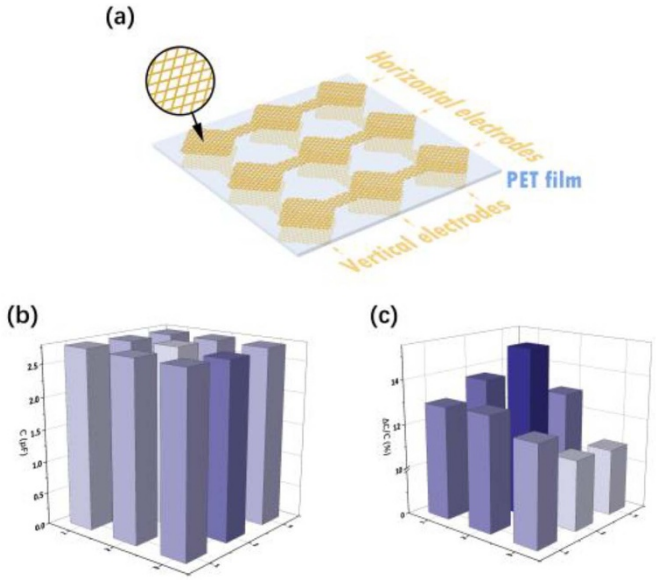

Figure 6. (a) Schematic diagram of the 3 × 3 array (b) The static capacitance distribution of the 3 × 3 array. (c) The distribution of proportion of capacitance change when the array is touched at the center.

3.2. Performance of touch sensing

The capacitance and touch response of the individual detectors were measured by Keysight 4980A. The static capacitance of a single sensor (before touch) was about 2.77pF, and there were subtle differences between different units. Figure 4(c) shows the capacitance change ($\frac{\Delta C}{C}$) when it was touched by different fingers in different cases, including wearing, not wearing rubber gloves, slight touch and full touch. The maximum ratio of capacitance change reached 41.8% when it is fully touched by a thumb without gloves, while the smallest, caused by the little finger's slight touch with gloves, was 13.2%.

3.3. Simulation of mesh capacitor

In a capacitive touch device, the capacitance of each touch unit has a significant influence on the response time of the device, so it is necessary to understand the influence of different structural parameters on the sensor's capacitance. Different structural parameters of the mesh touch sensor, such as width (w), period (d) and side length (l), were investigated via COMSOL Multiphysics. Two mesh capacitor models were constructed: one had a 60-degree mesh that was the same as the sensor we fabricated and the other had a 90-degree mesh containing a mesh of lines that are perpendicular to each other.

Figure 5(a) shows the relationship between C and w. The 60-degree structure can achieve a larger capacitance than the 90-degree structure, which is one of the reasons for adopting the diamond mesh structure mentioned in the design section. It also indicates that when w is close to d, meaning that the mesh is close to the metal plate, the capacitance values of the 90-degree and 60-degree structures tend to coincide, which is consistent with our expectation. Figure 5(b) shows that when d is much larger than w, the relationship between C and d slowly approaches 0 when d increases. In addition, the relationship between l and C is studied, and the results are shown in figure 5(c). As expected, when $\frac{w}{d}$ is $\frac{1}{35}$, much smaller than 1, the relationship between C and l^2 exhibits extreme linearity. This means the relationship between C and l has a simple quadratic relationship since l determines the area of the electrode, which indicates that the behavior of the mesh capacitor is similar to that of a typical capacitor. Surprisingly, when d is set as 35 times w and l is 33 times d, the capacitance values of the two structures have totally different behaviors as w increases, as shown in figure 5(d). In this case, the relationship between the capacitance value and w of the 60-degree structure exhibits very strong linearity, which can be used to design a flexible capacitive device in the future.

3.4. 3 × 3 touch sensor array

A 3 × 3 sensor array, as shown in figure 6(a), was used to demonstrate the sensor's touch function. As shown in figure 6(b), the static capacitances are basically the same. When the center of the array was touched, the capacitance of all the cells was affected, and the touch position could be concluded from the case where the capacitance was redistributed. Figure 6(c) shows the distribution of the rate change of capacitance ($\frac{\Delta C}{C}$), from which it can be determined that the touch-point is at the center of the array.

In summary, we have demonstrated a double-sided nanoimprint lithography method, and successfully fabricated a capacitive touch sensor based on Al mesh. This method has great potential for flexible electronics manufacturing.

Acknowledgments

This work was financially supported by the National Key R&D Program of China (Grant No. 2018YFB2200900) and National Natural Science Foundation of China (Grant No. 61775206). The fabrication work was partially carried out at the USTC Center for Micro and Nanoscale Research and Fabrication.

ORCID iD

Liang Wang https://orcid.org/0000-0003-2422-0916

References

[1] Ummartyotin S, Juntaro J, Sain M and Manuspiya H 2012 Development of transparent bacterial cellulose nanocomposite film as substrate for flexible organic light emitting diode (OLED) display *Ind. Crops Prod.* **35** 92–7
[2] Mishra R K, Hubble L J, Martín A, Kumar R, Barfidokht A, Kim J, Musameh M M, Kyratzis I L and Wang J 2017 Wearable flexible and stretchable glove biosensor for on-site detection of organophosphorus chemical threats *ACS Sensors* **2** 553–61
[3] Shin D H, Heo J H and Im S H 2017 Recent advances of flexible hybrid perovskite solar cells *J. Korean Phys. Soc.* **71** 593–607
[4] Han S T, Peng H, Sun Q, Venkatesh S, Chung K S, Lau S C, Zhou Y and Roy V 2017 An overview of the development of flexible sensors *Adv. Mater.* **29** 1700375
[5] Kumar A and Zhou C 2010 The race to replace tin-doped indium oxide: which material will win? *ACS Nano* **4** 11–4
[6] Kim D-J, Kim H-J, Seo K-W, Kim K-H, Kim T-W and Kim H-K 2015 Indium-free, highly transparent, flexible Cu 2 O/Cu/Cu 2 O mesh electrodes for flexible touch screen panels *Sci. Rep.* **5** 16838
[7] Kim K S, Zhao Y, Jang H, Lee S Y, Kim J M, Kim K S, Ahn J-H, Kim P, Choi J-Y and Hong B H 2009 Large-scale pattern growth of graphene films for stretchable transparent electrodes *Nature* **457** 706
[8] Lee J, Novoselov K S and Shin H S 2010 Interaction between metal and graphene: dependence on the layer number of graphene *ACS Nano* **5** 608–12
[9] Zeng X Y, Zhang Q K, Yu R M and Lu C Z 2010 A new transparent conductor: silver nanowire film buried at the surface of a transparent polymer *Adv. Mater.* **22** 4484–8
[10] Kim D-J, Shin H-I, Ko E-H, Kim K-H, Kim T-W and Kim H-K 2016 Roll-to-roll slot-die coating of 400 mm wide, flexible, transparent Ag nanowire films for flexible touch screen panels *Sci. Rep.* **6** 34322
[11] Son S, Park J E, Lee J, Yang M and Kang B 2016 Laser-assisted fabrication of single-layer flexible touch sensor *Sci. Rep.* **6** 34629
[12] Choi Y-M, Kim K-Y, Lee E, Jo J and Lee T-M 2015 Fabrication of a single-layer metal-mesh touchscreen sensor using reverse-offset printing *J. Inf. Dis.* **16** 37–41
[13] Elschner A and Lövenich W 2011 Solution-deposited PEDOT for transparent conductive applications *MRS Bulletin* **36** 794–8
[14] Kirchmeyer S and Reuter K 2005 Scientific importance, properties and growing applications of poly (3, 4-ethylenedioxythiophene) *J. Mater. Chem.* **15** 2077–88
[15] Argun A A, Cirpan A and Reynolds J R 2003 The first truly all-polymer electrochromic devices *Adv. Mater.* **15** 1338–41
[16] Gruner G 2006 Carbon nanotube films for transparent and plastic electronics *J. Mater. Chem.* **16** 3533–9
[17] Hecht D S, Hu L and Irvin G 2011 Emerging transparent electrodes based on thin films of carbon nanotubes, graphene, and metallic nanostructures *Adv. Mater.* **23** 1482–513
[18] Feng C, Liu K, Wu J S, Liu L, Cheng J S, Zhang Y, Sun Y, Li Q, Fan S and Jiang K 2010 Flexible, stretchable, transparent conducting films made from superaligned carbon nanotubes *Adv. Funct. Mater.* **20** 885–91
[19] Hong S, Yeo J, Kim G, Kim D, Lee H, Kwon J, Lee H, Lee P and Ko S H 2013 Nonvacuum, maskless fabrication of a flexible metal grid transparent conductor by low-temperature selective laser sintering of nanoparticle ink *ACS Nano* **7** 5024–31
[20] Kim W-K, Lee S, Lee D H, Park I H, Bae J S, Lee T W, Kim J-Y, Park J H, Cho Y C and Cho C R 2015 Cu mesh for flexible transparent conductive electrodes *Sci. Rep.* **5** 10715
[21] Kang M G, Kim M S, Kim J and Guo L J 2008 Organic solar cells using nanoimprinted transparent metal electrodes *Adv. Mater.* **20** 4408–13
[22] Xu K, Luo H, Qin J, Yang M, Guo S and Wang L 2018 Flexible devices fabricated by a plate-to-roll nanoimprint lithography system *Nanotechnology* **30** 075301
[23] Tan H, Gilbertson A and Chou S Y 1998 Roller nanoimprint lithography *J. Vacuum Sci. Technol.* B **16** 3926–8
[24] Hauser H, Michl B, Schwarzkopf S, Kübler V, Müller C, Hermle M and Bläsi B 2012 Honeycomb texturing of silicon via nanoimprint lithography for solar cell applications *IEEE J. Photovolt.* **2** 114–22
[25] Ahn S H and Guo L J 2008 High-speed roll-to-roll nanoimprint lithography on flexible plastic substrates *Adv. Mater.* **20** 2044–9
[26] Ahn S H and Guo L J 2009 Large-area roll-to-roll and roll-to-plate nanoimprint lithography: a step toward high-throughput application of continuous nanoimprinting *ACS Nano* **3** 2304–10
[27] Philips'Gloeilampenfabrieken O 1958 A method of measuring specific resistivity and Hall effect of discs of arbitrary shape *Philips Res. Rep.* **13** 1–9
[28] Nair N M, Daniel K, Vadali S C, Ray D and Swaminathan P 2019 Direct writing of silver nanowire-based ink for flexible transparent capacitive touch pad *Flex. Print. Electron.* **4** 045001